THE ASTROPHYSICAL JOURNAL, 512:L43–L46, 1999 February 10

STRONG APERIODIC X-RAY VARIABILITY AND QUASI-PERIODIC OSCILLATION IN X-RAY NOVA XTE J1550−564

WEI CUI,[1] SHUANG NAN ZHANG,[2] WAN CHEN,[3,4] AND EDWARD H. MORGAN[1]
Received 1998 November 3; accepted 1998 December 8; published 1998 December 23

ABSTRACT

We report the discovery of strong aperiodic X-ray variability and quasi-periodic oscillation (QPO) in the X-ray light curves of a new X-ray nova, XTE J1550−564, and the evolution of the observed temporal properties during the rise of the recent X-ray outburst. The power spectral analysis of the first observation reveals strong aperiodic X-ray variability of the source (∼28%) as well as the presence of a QPO at ∼82 mHz with fractional rms amplitude ∼14% over the 2–60 keV energy range. Also apparent is the first harmonic of the QPO with the amplitude ∼9%. As the X-ray flux increases, the source tends to become less variable, and the QPO frequency increases rapidly, from 82 mHz to 4 Hz, over the flux (2–50 keV) range of 1.73–5.75 × 10^{-8} ergs cm^{-2} s^{-1}. The amplitude of the fundamental component of the QPO varies little, while that of the harmonic follows a decreasing trend. The fundamental component strengthens toward high energies, while its harmonic weakens. Initially, the power spectrum is roughly flat at low frequencies and turns into a power law at high frequencies, with the QPO harmonic sitting roughly at the break. In later observations, however, the high-frequency portion of the continuum can actually be better described by a broken power law (as opposed to a simple power law). This effect becomes more apparent at higher energies. The overall amplitude of the continuum shows a similar energy dependence to that of the fundamental component of the QPO. Strong rapid X-ray variability, as well as a hard energy spectrum, makes XTE J1550−564 a good black hole candidate. We compare its temporal properties with those of other black hole candidates.

Subject headings: binaries: general — stars: individual (XTE J1550−564) — X-rays: stars

1. INTRODUCTION

A new X-ray nova designated as XTE J1550−564 was discovered by the All-Sky Monitor (ASM) aboard the *Rossi X-ray Timing Explorer* (*RXTE*) on 1998 September 7 (Smith 1998). A possible optical counterpart was soon identified (Orosz, Bailyn, & Jain 1998), and a variable radio source was subsequently found at the optical position (Campbell-Wilson et al. 1998). These identifications were later confirmed by a much improved error box on the position of XTE J1550−564, derived from an *ASCA* observation of the source (Marshall et al. 1998).

Shortly after the ASM discovery of XTE J1550−564, we initiated a daily monitoring campaign with the more sensitive detectors aboard *RXTE*: the Proportional Counter Array (PCA) and High-Energy X-ray Timing Experiment (HEXTE). This is a program that we have set up to study the X-ray properties of soft X-ray transients during the rise of an X-ray outburst. In this Letter, we report the discovery of strong aperiodic X-ray variability and quasi-periodic oscillation (QPO) in the X-ray light curves of XTE J1550−564 as well as the evolution of the observed temporal properties throughout the rising phase of the outburst.

2. OBSERVATIONS

Figure 1 shows a portion of the long-term ASM light curve of XTE J1550−564 that highlights the rising phase of the recent outburst. The rising phase begins with a fast rise (with *e*-folding time less than 1 day) followed by a slow rise (with *e*-folding time ∼1 week). During the fast rise, the soft hardness ratio appears to decrease, while the hard ratio appears to increase. The X-ray spectrum softens progressively during the slow rise, until the source settles into a soft state.

The times of our pointed *RXTE* observations are indicated in Figure 1. Note that the first two observations were made during the fast rise. For this study, we will use only the PCA data to investigate rapid X-ray variability of XTE J1550−564. There are a total of 14 observations, covering the entire rising phase of the outburst at a typical rate of once or twice per day. The effective exposure time varies in the range of 1.2–6 ks. The first observation was a direct spacecraft slew to the source, so it inherited the data modes (GoodXenon with 16 s readout time) from the prior observation of a faint object. As a result, the data buffers were overfilled due to the high count rate of XTE J1550−564, causing significant gaps in the GoodXenon data. These data modes were replaced, in the second observation, by the combination of an Event mode with ∼62 μs timing resolution and a Binned mode with ∼8 ms timing resolution, which together cover the entire PCA energy band (a Single Bit mode with ∼62 μs timing resolution was also used, covering the same energy range as the Binned mode). We subsequently optimized the data modes further for higher timing resolution (at the expense of energy resolution): an Event mode with ∼16 μs timing resolution and a Binned mode with ∼4 ms timing resolution.

3. DATA ANALYSIS AND RESULTS

We have carried out preliminary spectral analysis. Throughout the rising phase, the X-ray spectrum can be roughly described by a multicolor disk ("diskbb" in XSPEC) plus a power law. The inclusion of a gradual rollover (at 16–18 keV) of the power law and a Gaussian component (between 6 and 7 keV)

[1] Center for Space Research, Massachusetts Institute of Technology, Cambridge, MA 02139; cui@space.mit.edu, ehm@space.mit.edu.
[2] Department of Physics, University of Alabama in Huntsville, Huntsville, AL 35899; zhangsn@email.uah.edu.
[3] NASA/Goddard Space Flight Center, Code 661, Greenbelt, MD 20771; chen@milkyway.gsfc.nasa.gov.
[4] Also at Department of Astronomy, University of Maryland, College Park, MD.

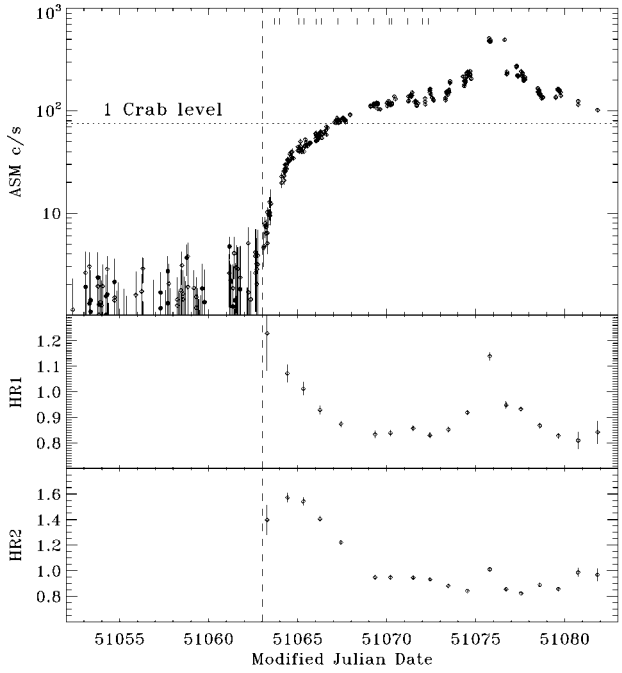

FIG. 1.—ASM light curves of XTE J1550−564. *Top:* Each data point is derived from a 90 s measurement, with negative values shown as filled circles for completeness. The dashed line indicates roughly the time (MJD 51063 or 1998 September 7 UT) when the outburst started. For reference, the dotted line shows the ASM count rate of the Crab Nebula. The short vertical lines at the top indicate the times of the pointed *RXTE* observations reported in this Letter. *Middle:* Soft hardness ratio is defined as the radio of the count rate in the 3.0–4.8 keV band to that in the 1.3–3.0 keV band. Shown are the daily averaged results. *Bottom:* Hard hardness ratio is defined as the radio of the count rate in the 4.8–12 keV band to that in the 3.0–4.8 keV band.

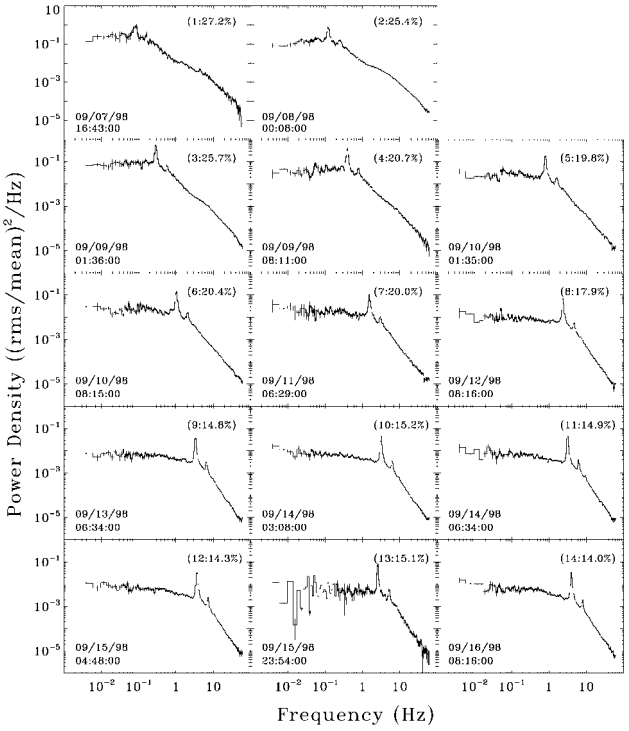

FIG. 2.—Power density spectrum. The start time (in UT) of each observation is shown, as is the overall fractional rms amplitude of the continuum over the frequency range 0.001–64 Hz.

significantly improves the fit. As the source brightens, the soft component strengthens and the power law steepens, with the photon index varying from ∼1.3 to ∼2.4. Detailed spectral analysis (including the HEXTE data) will be presented in a future paper. Here, we simply use the preliminary model to compute *observed* X-ray flux (2–50 keV) for each observation.

For timing analysis, the high-resolution data were first rebinned to 2^{-7} s in order to facilitate comparison of results between observations with data modes of different timing resolution. The data sets were then combined to cover the entire PCA energy band. A fast-Fourier transform (FFT) was carried out for every 256 s segment (with the mean subtracted and gaps filled with 0 prior to FFT) of each observation. Individual power density spectra were weighted and co-added to obtain the average power density spectrum (PDS) for that observation. The results are shown in Figure 2. Note that the data gaps in observation 1 significantly affect the low-frequency portion of the PDS, so what is shown (up to 4 Hz) was actually constructed from the Standard 1 data (which is free of any data gaps).

In the first four observations, the PDS continuum is approximately flat at low frequencies and falls off following a power law at high frequencies. The presence of a pair of QPOs is apparent, with the higher frequency one sitting roughly at the break. There also exists a broad bump between 1 and 10 Hz. We modeled the continuum as described, using Lorentzian functions for the QPOs and the broad bump. The results indicate that the QPO pair is consistent with being harmonics of the same oscillation (Fig. 3). In some cases, the second harmonic also becomes discernible (Fig. 2). As the source brightens, the power-law portion of the PDS steepens (with the index dropping from ∼−1.5 to ∼−1.7). Starting from observation 5, the PDS can actually be better described by a broken power law at high frequencies, following the flat component. This effect becomes more apparent at higher energies (see Fig. 4). The high-frequency portion of the PDS continues to steepen before

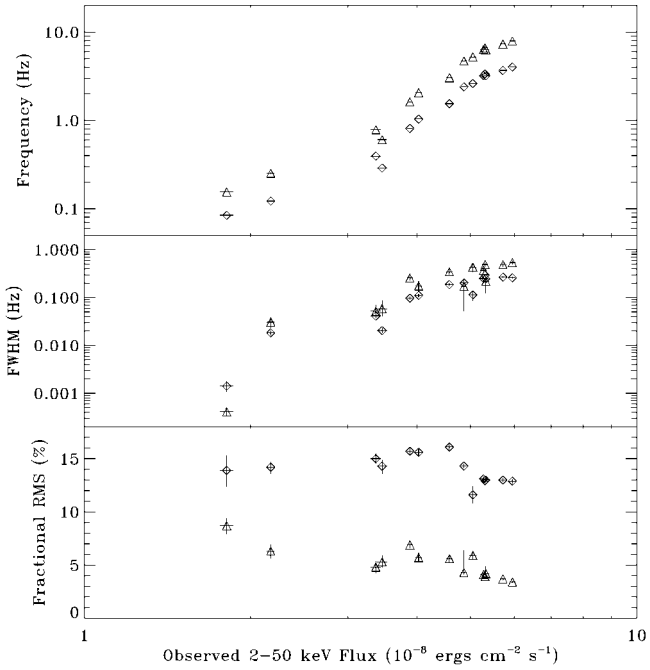

FIG. 3.—Evolution of the QPO during the rising phase of the outburst. Diamonds show the fundamental component, and triangles show the first harmonic.

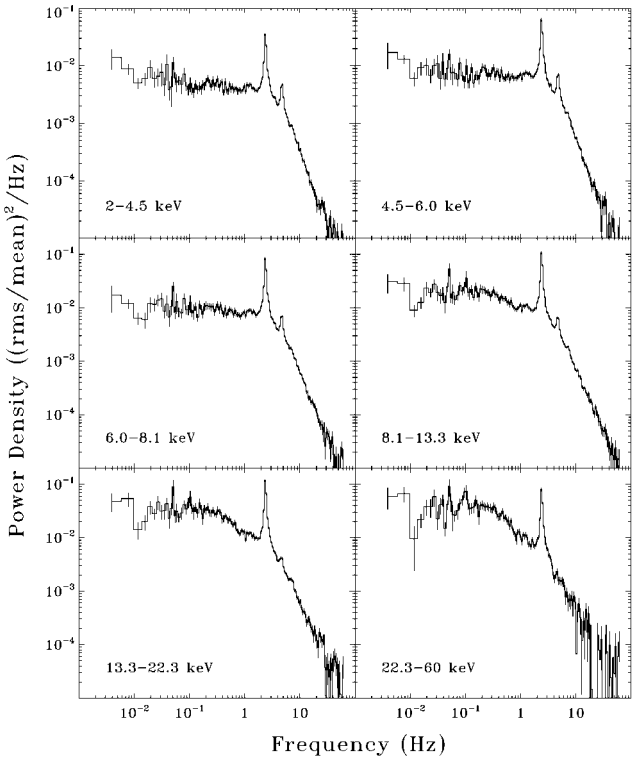

FIG. 4.—Power density spectra in six energy bands. This example is for observation 8, but the results are similar for all observations. Note the weakening of the first harmonic of the QPO toward high energies, as well as the change in the continuum shape.

it saturates at a power-law index of ~ -2.4 in observation 8. The break between the two power laws roughly coincides with the first QPO harmonic throughout the entire period, while the cutoff of the flat component moves little. The index of the shallower power law varies in the range ~ -0.8 to -0.5. Overall, the source becomes less variable (in terms of the fractional amplitude of the continuum; Fig. 2), as it becomes brighter.

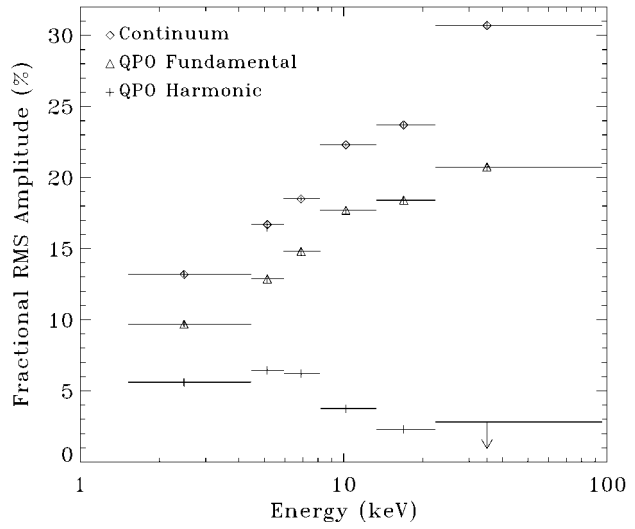

FIG. 5.—Energy dependence of the QPO and the PDS continuum. As in Fig. 4, the results of observation 8 are shown to illustrate the general dependence. The results are plotted at the effective energy for each band (as defined in the text). A 3 σ upper limit is shown for the case of nondetection.

The QPO frequency rises steeply with the increase of X-ray flux, as shown in Figure 3, roughly following a power law with index of $+4.2$ (although it seems to show sign of leveling off at high fluxes). While the fractional rms amplitude of the fundamental QPO varies little, that of the first harmonic follows a decreasing trend. There does not appear to be any qualitative difference in the QPO properties between the periods of fast rise and slow rise.

To investigate energy dependence of the temporal properties, we chose six energy bands: 2–4.5, 4.5–6.0, 6.0–8.1, 8.1–13.3, 13.3–22.3, and 22.3–60 keV. Figure 4 shows the PDS in each of these bands, using observation 8 as an example (the results are similar for all observations). We then defined an "effective" energy for each energy band:

$$E_{\rm eff} = \frac{\sum_i \int ER(i, E)S(E)dE}{\sum_i \int R(i, E)S(E)dE}, \quad (1)$$

where $S(E)$ is the photon flux at energy E, and $R(i, E)$ is the detector response matrix that distributes photons at energy E to counts in each pulse-height channel i; energy integrals are computed over a chosen energy band, while all pulse-height channels are summed up. We fit the PDS, similarly as before, in each band. Figure 5 summarizes the results as a function of the effective energy. Both the continuum and the fundamental component of the QPO strengthens toward high energies, in terms of their fractional rms amplitudes, while the QPO harmonic weakens. Our results at high energies are in general agreement with those from the BATSE observations (Finger, Dieters, & Wilson 1998).

As for the broad bump, it is initially centered at ~2.4 Hz with FWHM ~9 Hz and fractional rms amplitude 17%–19% during the fast rise (see Fig. 1). The feature begins to weaken during the slow rise. The fractional rms amplitude drops to ~10% and ~6% in observations 3 and 4, respectively. In the meantime, the centroid frequency increases to ~4.0 and ~6.4 Hz, respectively. The feature becomes undetectable in subsequent observations.

4. DISCUSSION

The rise of XTE J1550−564 shows a more complicated profile than the canonical exponential rise (see Chen, Shrader, & Livio 1997 for a compilation of outburst profiles). During the fast rise, the source brightened at nearly all wavelengths (soft and hard X-rays, optical, and radio). This is consistent with a sudden surge in the mass accretion rate at onset of the outburst, as generally thought (see review by King 1995). During the slow rise, however, the ASM flux (1.3–12 keV) becomes *anticorrelated* with the BATSE flux (25–200 keV),[5] similar to Cyg X-1 during its transition between the hard and soft states (Cui et al. 1997a; Zhang et al. 1997). It is interesting to note that the soft and hard fluxes became *positively* correlated again during a giant flare around MJD 51076. In fact, the BATSE flux reached nearly the same level during the flare as that at the end of the fast rise. Perhaps the same physical processes operate in initiating the outburst and in setting off the flare.

The observed rapid X-ray variability and hard energy spectrum make XTE J1550−564 a likely black hole candidate (BHC). Prior to the launch of *RXTE*, QPOs in BHCs were

[5] See http://www.batse.msfc.nasa.gov/data/occult/fluxhistories for BATSE measurements.

observed only at very low frequencies (less than 1 Hz, except for the "very high state" QPOs at a few hertz observed only on two occasions; see van der Klis 1995). *RXTE* has pushed the discovery space up to hundreds of hertz (see Cui 1998). The PDS of XTE J1550−564 bears resemblance to that of GRS 1915+105 in the "low-hard" state (Morgan, Remillard, & Greiner 1997), where a strong QPO was detected, as well as its first harmonic in some cases. Following Morgan et al. (1997), we have tracked individual pulses of the QPO (fundamental component) in XTE J1550−564. The results imply that the QPO represents a random walk in the oscillation phase, like its counterpart in GRS 1915+105. However, while the QPO frequency varies with X-ray flux for both sources, the exact frequency-flux correlation is different *quantitatively* (comparing our results with those of Chen, Swank, & Taam 1997). In general, the presence of QPOs seems to be characteristic of BHCs during the transitions between the hard and soft states (Cui 1998). Therefore, the slow rise of XTE J1550−564 may indeed represent such a transition, as also indicated by the observed spectral evolution (see Fig. 1). On the other hand, the canonical $1/f$ PDS shape for the soft state (van der Klis 1995; Cui 1998) was not seen here.

XTE J1550−564 has offered the best case of tracking a QPO over a wide range of X-ray flux. Previous studies were usually hindered by the ambiguity in "labeling" a moving QPO as the X-ray flux varies, due to insufficient coverage of the phenomenon. After all, QPOs are often transient phenomena; different QPOs can be present in different observations for a particular source. Here, XTE J1550−564 was monitored at least once a day so the evolution of the QPO could be closely followed. The presence of the strong harmonic component also helps uniquely identify the feature. Therefore, the observed correlation between the QPO properties and X-ray flux is reliable. Such a correlation seems to suggest an origin for the QPOs in XTE J1550−564 that is different from that of the 67 or 300 Hz QPOs in microquasars, whose frequency is stable against any variation in the X-ray flux, and different from that of those QPOs (in BHCs in general) whose frequency decreases with the flux increase. It is worth commenting that the reported weak QPO at 184 Hz during the giant flare (McClintock et al. 1998) is probably not of the same type, since an extrapolation of the best-fit power law of the frequency-flux relation (Fig. 3) would require a flux increase only by a factor of ~2.5 during the flare. This is much less than the observed increase (by a factor of ~3.9 in the ASM count rate, thus, more in the flux because the energy spectrum hardens during the flare). Moreover, although the QPO seen here broadens as the source becomes brighter, the Q-value ($\equiv f_{\rm qpo}/{\rm FWHM}$) tends to increase mildly, reaching ~15 (derived from Fig. 3), which is much larger than that of the 184 Hz QPO (~4).

Like most QPOs observed in BHCs (Cui 1998, and references therein), the fundamental component of the QPO in XTE J1550−564 strengthens toward high energies. Interestingly, however, the QPO harmonic becomes weaker, which is again similar to the low hard state QPO in GRS 1915+105 as well as to the very high state QPOs (Belloni et al. 1997; Takizawa et al. 1997). The energy dependence of QPO amplitudes has not been emphasized enough but might hold the key to our understanding of the origin of these QPOs (Cui 1998). The dependence seems to rule out the possibility that these QPOs are produced by any oscillatory processes in a standard thin accretion disk (Shakura & Sunyaev 1973), since the X-ray emission from such a disk is very soft (less than a few keV). The hard X-ray emission is generally thought to be the product of energetic electrons (thermal or nonthermal) inverse Compton scattering soft photons in the system. The scattering electrons then serve as a "low-pass filter" to any intrinsic variability associated with the seed photons (Cui et al. 1997a; Kazanas, Hua, & Titarchuk 1997). Therefore, the increase of the PDS break frequency as the source brightens (see Fig. 2) perhaps implies a decrease in the size of the Comptonizing region, as is being suggested for Cyg X-1 during the state transition (Cui et al. 1997a, 1997b). The QPO might simply originate in the Comptonizing region, due to oscillation in the density and/or energy distribution of hot electrons during the rising phase of the outburst (Cui et al. 1997b; Kazanas et al. 1997; Titarchuk, Lapidus, & Muslimov 1998). It remains to be seen whether the observed properties, such as dependence of the QPO properties both on photon energy and X-ray flux (i.e., mass accretion rate), can be accounted for *quantitatively* in this scenario. The origins of QPOs in BHCs are still poorly understood at present (van der Klis 1995; Cui 1998). Few detailed models exist due to the lack of data. Hopefully, more and better data provided by missions like *RXTE* will soon lead to quantitative modeling of the phenomena.

We thank Michiel van der Klis for useful comments. This work is supported in part by NASA grants NAS5-30612 and NAG5-7484.

REFERENCES

Belloni, T., et al. 1997, A&A, 322, 857
Campbell-Wilson, D., McIntyre, V., Hunstead, R., & Green, A. 1998, IAU Circ. 7010
Chen, W., Shrader, C. R., & Livio, M. 1997, ApJ, 491, 312
Chen, X., Swank, J. H., & Taam, R. E. 1997, ApJ, 477, L41
Cui, W. 1998, in High-Energy Processes in Accreting Black Holes, ed. J. Poutanen & R. Svensson (San Francisco: PASP), in press (astro-ph/9809408)
Cui, W., Heindl, W. A., Rothschild, R. E., Zhang, S. N., Jahoda, K., & Focke, W. 1997a, ApJ, 474, L57
Cui, W., Zhang, S. N., Focke, W., & Swank, J. 1997b, ApJ, 484, 383
Finger, M. H., Dieters, S. W., & Wilson, R. B. 1998, IAU Circ. 7010
Kazanas, D., Hua, X.-M., & Titarchuk, L. 1997, ApJ, 480, 735
King, A. R. 1995, in X-ray Binaries, ed. W. H. G. Lewin, J. van Paradijs, & E. P. J. van den Heuvel (Cambridge: Cambridge Univ. Press), 419
Marshall, F. E., Smith, D. A., Dotani, T., & Ueda, Y. 1998, IAU Circ. 7013
McClintock, J., et al. 1998, IAU Circ. 7025
Morgan, E. H., Remillard, R. A., & Greiner, J. 1997, ApJ, 482, 993
Orosz, J., Bailyn, C., & Jain, R. 1998, IAU Circ. 7009
Shakura, N. I., & Sunyaev, R. A. 1973, A&A, 24, 337
Smith, D. A. 1998, IAU Circ. 7008
Takizawa, M., et al. 1997, ApJ, 489, 272
Titarchuk, L., Lapidus, I., & Muslimov, A. 1998, ApJ, 499, 315
van der Klis, M. 1995, in X-ray Binaries, ed. W. H. G. Lewin, J. van Paradijs, & E. P. J. van den Heuvel (Cambridge: Cambridge Univ. Press), 252
Zhang, S. N., Cui, W., Harmon, B. A., Paciesas, W. S., Remillard, R. E., & van Paradijs, J. 1997, ApJ, 477, L95